ELSEVIER

Journal of Organometallic Chemistry 507 (1996) 163–178

Journal of Organometallic Chemistry

High nuclearity ruthenium carbonyl cluster chemistry III ☆. Synthesis of $[Ru_{10}(\mu\text{-H})(\mu_6\text{-C})(CO)_{24}]^-$, its reactivity towards triphenylphosphine and ligand dynamics of the resulting decaruthenium anionic clusters

Marie P. Cifuentes [a], Mark G. Humphrey [b,*], Brian W. Skelton [c], Allan H. White [c]

[a] *Department of Chemistry, University of New England, Armidale, New South Wales 2351, Australia*
[b] *Department of Chemistry, Australian National University, Canberra, Australian Capital Territory 0200, Australia*
[c] *Department of Chemistry, University of Western Australia, Nedlands, Western Australia 6907, Australia*

Received 11 April 1995

Abstract

Thermolysis of $Ru_3(\mu\text{-H})(\mu\text{-NC}_5H_4)(CO)_{10}$ in refluxing chlorobenzene affords $[Ru_2(\mu\text{-H})(\mu\text{-NC}_5H_4)_2(CO)_4(NC_5H_5)_2][Ru_{10}(\mu\text{-H})(\mu_6\text{-C})(CO)_{24}]$ (**1a**) in excellent yield. The results of a structural study of **1a** are consistent with the hydride occupying an edge-bridging site at an apex of the "giant tetrahedron". Thermolysis of $Ru_3(\mu\text{-H})(\mu\text{-NC}_5H_4)(CO)_{10}$ with $[PPh_4][BF_4]$ in chlorobenzene affords the cluster $[PPh_4][Ru_{10}(\mu\text{-H})(\mu_6\text{-C})(CO)_{24}]$ (**1b**) in moderate yield. Compound **1a** reacts immediately with 1 equiv. of triphenylphosphine at room temperature to afford the monosubstituted cluster $[Ru_2(\mu\text{-H})(\mu\text{-NC}_5H_4)_2(CO)_4(NC_5H_5)_2][Ru_{10}(\mu\text{-H})(\mu_6\text{-C})(CO)_{23}(PPh_3)]$ (**2a**) in high yield; the crystal structure of **2a** and NMR studies show that ligand substitution occurs at the apical ruthenium associated with the hydride ligand. Further reaction with triphenylphosphine at room temperature affords successively the complexes $[Ru_{10}(\mu\text{-H})(\mu_6\text{-C})(CO)_{24-x}(PPh_3)_x]^-$ with $x = 2$ (**3a**) and 3 (**4a**); the tetrasubstituted cluster ($x = 4$, **5c**) is obtained as its $[Ru_2(\mu\text{-H})(\mu\text{-NC}_5H_4)_2(CO)_4(PPh_3)_2]^+$ salt following a short reflux in acetone. In each case, substitution occurs at the apical ruthenium atoms. Hydride and CO fluxionality in the five cluster anions was investigated by ^{13}C EXSY experiments. Compound **1a** exhibits complete hydride fluxionality between the four apices at low temperature, while **5c** shows similar behaviour at room temperature. CO fluxionality increases with phosphine substitution, reaching a maximum at the bis-substituted cluster, and becoming less facile on the tris- and tetrakis-substituted cluster anions. Compound **1b** reacts in a similar manner with triphenylphosphine to form an analogous series of complexes. Attempted metathesis of preformed **1a** by reaction with [PPN]Cl was unsuccessful; instead, conversion to $[PPN]_2[Ru_{10}(\mu_6\text{-C})(CO)_{24}]$ occurs.

Keywords: Ruthenium; Carbonyl; Clusters; Fluxionality; Crystal structures

1. Introduction

We have been interested in modelling the hydrotreatment of coal-derived fuels, and have recently reported ruthenium cluster chemistry of piperidine- [2], pyridine- [3] and phenol- [4,5] derived ligands. In an attempt to vary the coordination mode of an edge-bridging pyridyl ligand, we have investigated the thermolysis of $Ru_3(\mu\text{-H})(\mu\text{-NC}_5H_4)(CO)_{10}$. Surprisingly, the decaruthenium cluster anion $[Ru_{10}(\mu\text{-H})(\mu_6\text{-C})(CO)_{24}]^-$ is obtained in excellent yield as its $[Ru_2(\mu\text{-H})(\mu\text{-NC}_5H_4)_2(CO)_4(NC_5H_5)_2]^+$ salt. High-nuclearity (hydrido)ruthenium clusters are rare [6]; the only previous reports are of $[H_2Ru_{10}(CO)_{25}]^{2-}$ [7], $[HRu_{11}(CO)_{27}]^{3-}$ [8] and $[HRu_{10}C(CO)_{24}]^-$ [9], obtained in reported yields of 15%, 20% and 15%, respectively. The low yield and tedious preparation of the last-mentioned in particular (refluxing $Ru_3(CO)_{12}$ in mesitylene for 3–5 days, followed by chromatography of a mixture of at least six products) has hindered reactivity studies. We report

☆ For Part II, see Ref. [1].
* Corresponding author.

Elsevier Science S.A.
SSDI 0022-328X(95)05693-9

below the preparation of $[Ru_{10}(\mu\text{-H})(\mu_6\text{-C})(CO)_{24}]^-$ as both $[Ru_2(\mu\text{-H})(\mu\text{-}NC_5H_4)_2(CO)_4(NC_5H_5)_2]^+$ and $[PPh_4]^+$ salts, including a structural characterization of the former, studies of their reactivity towards triphenylphosphine, some comments on the cell packing in such clusters and CO fluxionality studies of the (hydrido)decaruthenium anionic clusters. Some of these results have been briefly reported in previous papers [1,10].

2. Results and discussion

2.1. Synthesis of $[Ru_2(\mu\text{-H})(\mu\text{-}NC_5H_4)_2(CO)_4(NC_5H_5)_2][Ru_{10}(\mu\text{-H})(\mu_6\text{-C})(CO)_{24}]$ (1a)

Refluxing a solution of $Ru_3(\mu\text{-H})(\mu\text{-}NC_5H_4)(CO)_{10}$ in chlorobenzene gave a black solution within 40–90

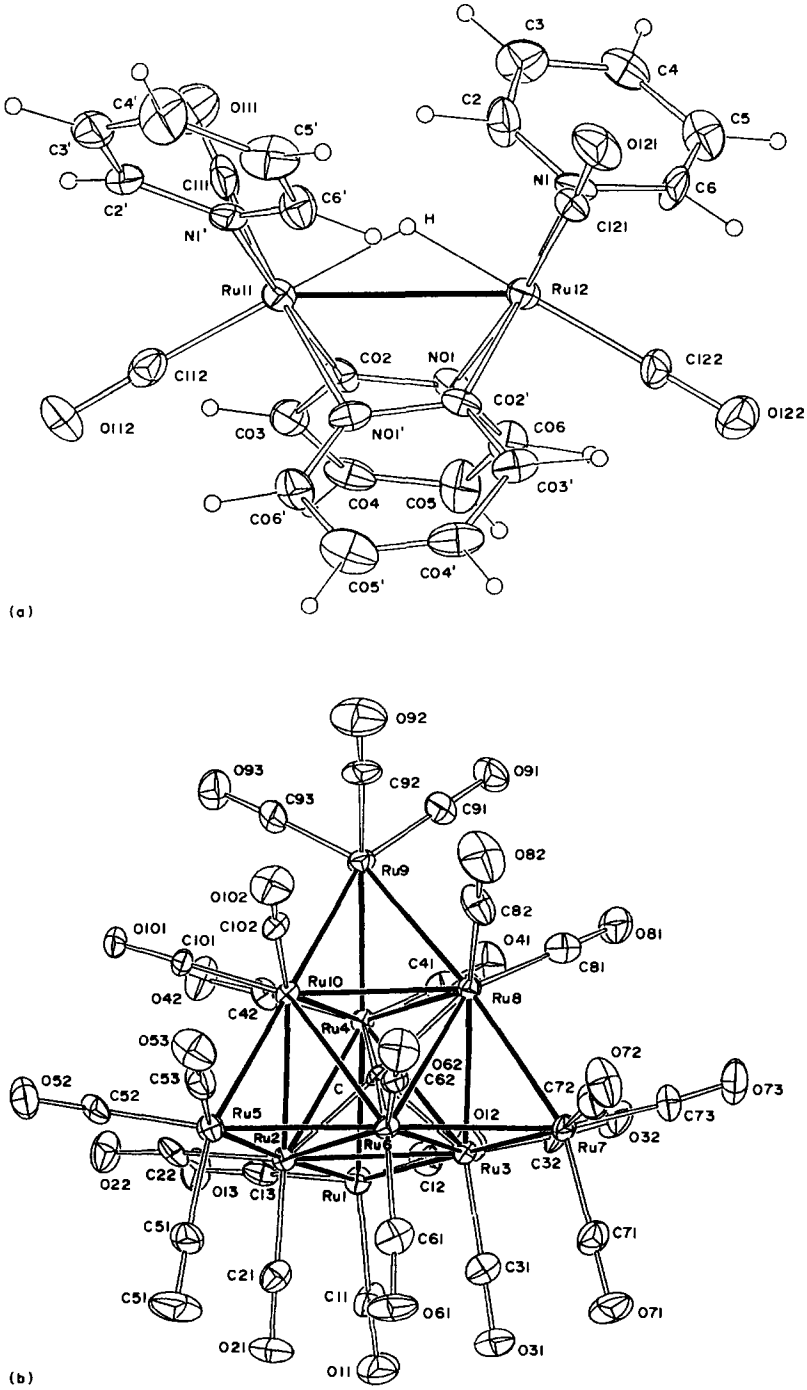

Fig. 1. ORTEP plots of (a) the cation and (b) the anion geometry in $[Ru_2(\mu\text{-H})(\mu\text{-}NC_5H_4)_2(CO)_4(NC_5H_5)_2][Ru_{10}(\mu\text{-H})(\mu_6\text{-C})(CO)_{24}]$ (1a). 20% thermal envelopes are shown for the non-hydrogen atoms. Hydrogen atoms have arbitrary radii of 0.1 Å.

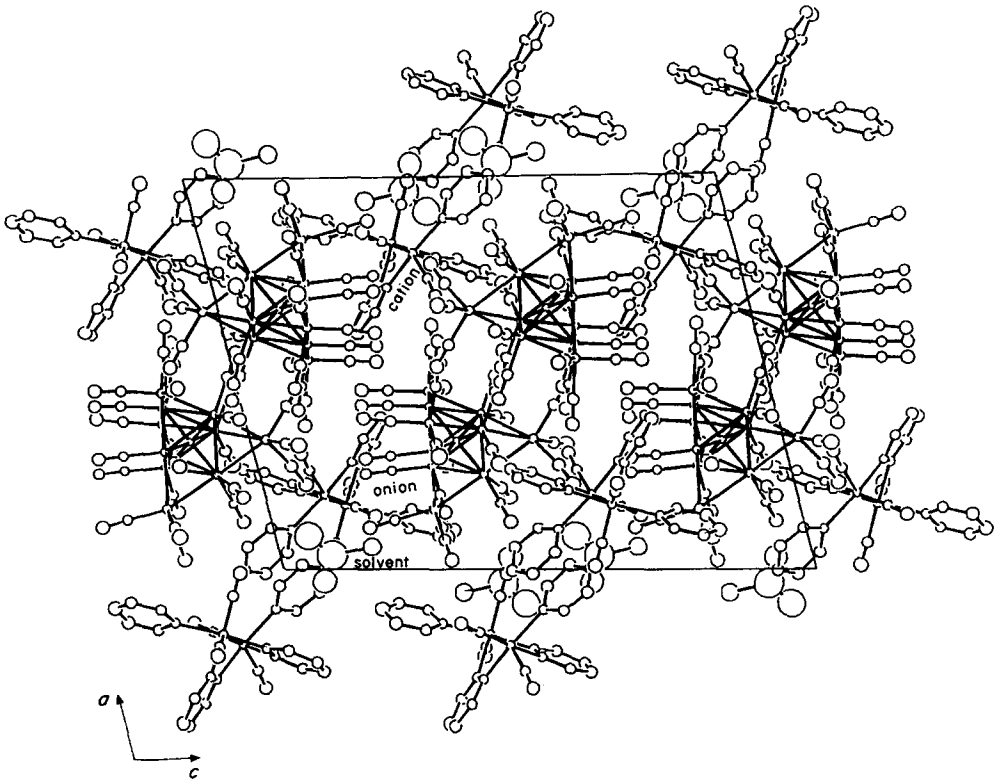

Fig. 2. Unit cell for **1a**.

min, and this was filtered and reduced to dryness in vacuo. Crystallization of the resulting residue from acetone afforded green–black crystals, identified as $[Ru_2(\mu\text{-}H)(\mu\text{-}NC_5H_4)_2(CO)_4(NC_5H_5)_2][Ru_{10}(\mu\text{-}H)(\mu_6\text{-}C)(CO)_{24}]$ (**1a**) by a combination of IR, ^1H, ^{13}C NMR and FAB-MS and satisfactory microanalyses, and confirmed by a single-crystal X-ray diffraction study. Considering the change in nuclearity, the reaction is remarkably clean, with no evidence for other carbonyl-containing products. Mechanistic speculation about the formation of **1a** from $Ru_3(\mu\text{-}H)(\mu\text{-}NC_5H_4)(CO)_{10}$ is not warranted at this stage; monitoring of the reaction by IR and ^1H NMR failed to reveal evidence for any reaction intermediates.

The solution IR spectrum of **1a** (ν(CO) 2052 (s), 2009 (m) 1997 (m, sh) cm^{-1}) and a resonance in the hydride region of the ^1H NMR spectrum (-13.55 ppm) are similar to those reported previously for $[HRu_{10}C(CO)_{24}]^-$ [9]; the characteristic carbide resonance was observed at 374.6 ppm in the ^{13}C NMR spectrum. Signals in the ^1H and ^{13}C NMR spectra are consistent with the presence of the hydrido (-10.74 ppm), pyridine and pyridyl ligands of the diruthenium cation $[Ru_2(\mu\text{-}H)(\mu\text{-}NC_5H_4)_2(CO)_4(NC_5H_5)_2]^+$. This unusual cation is related to $Ru_2(\mu\text{-}NC_5H_4)_2(CO)_6$, obtained as a mixture of head-to-head and head-to-tail isomers by Cockerton and Deeming [11] by heating $Ru_3(CO)_{12}$ with pyridine. Although the spectral data are consistent with the formulation $[Ru_2(\mu\text{-}H)(\mu\text{-}NC_5H_4)_2(CO)_4(NC_5H_5)_2][HRu_{10}C(CO)_{24}]$, a single-crystal X-ray diffraction study was undertaken to resolve questions regarding (i) the presence of possible isomers of the cation, such as were observed in $Ru_2(\mu\text{-}NC_5H_4)_2(CO)_6$, (ii) the postulated location of the hydrido ligand in the anion in an interstitial tetrahedral

Table 1
Summary of crystallographic and refinement data for **1a**

Formula	$C_{49}H_{20}N_4O_{28}Ru_{12}\cdot CH_2Cl_2$
M	2410.5
Crystal system	Monoclinic
Space group	$P2_1/c$
a (Å)	18.163(8)
b (Å)	15.934(9)
c (Å)	23.75(1)
β (°)	103.62(4)
V (Å^3)	6679(6)
Z	4
D_x (g cm^{-3})	2.40
$\mu_{Mo\ K\alpha}$ (cm^{-1})	27.9
Specimen (mm)	$0.08\times0.12\times0.18$
A^* min, max	1.23, 1.50
$F(000)$	4544
$2\theta_{max}$ (°)	50
N	11442
N_0	4882
R	0.048
R_w	0.039

A cautious and extensive exposition of the processing of this structure is given in Ref. [10] and is not repeated here

Table 2
Atomic coordinates and (equivalent) isotropic thermal parameters for **1a**

Atom	x	y	z	U_{eq} (Å^2)
Ru(1)	0.45885(9)	0.60133(9)	0.35428(6)	0.0433(6)
Ru(2)	0.30611(9)	0.64279(8)	0.33133(5)	0.0355(5)
Ru(3)	0.40213(9)	0.67031(8)	0.44355(5)	0.0343(5)
Ru(4)	0.42061(8)	0.76953(9)	0.34834(5)	0.0349(5)
Ru(5)	0.15563(9)	0.69435(9)	0.30836(6)	0.0452(6)
Ru(6)	0.24504(9)	0.71743(8)	0.41974(6)	0.0359(6)
Ru(7)	0.33746(9)	0.73668(9)	0.52946(5)	0.0421(6)
Ru(8)	0.36182(9)	0.84336(8)	0.43777(5)	0.0347(6)
Ru(9)	0.37820(9)	0.93619(9)	0.34018(6)	0.0429(6)
Ru(10)	0.26596(8)	0.81691(8)	0.32485(5)	0.0348(5)
Ru(11)	0.83311(9)	0.69887(9)	0.35561(6)	0.0417(6)
Ru(12)	0.80761(9)	0.87355(9)	0.38933(6)	0.0385(6)
C(11)	0.465(1)	0.487(1)	0.3743(7)	0.066(9)
O(11)	0.4705(9)	0.4195(7)	0.3874(6)	0.099(8)
C(12)	0.562(1)	0.613(1)	0.3775(8)	0.065(9)
O(12)	0.6264(7)	0.6220(8)	0.3917(5)	0.087(7)
C(13)	0.463(1)	0.5825(9)	0.2784(7)	0.053(8)
O(13)	0.4644(8)	0.5693(8)	0.2299(4)	0.083(7)
C(21)	0.280(1)	0.532(1)	0.3440(7)	0.058(8)
O(21)	0.2676(9)	0.4622(7)	0.3520(6)	0.100(8)
C(22)	0.2944(9)	0.625(1)	0.2511(6)	0.045(7)
O(22)	0.2871(8)	0.6108(8)	0.2032(5)	0.081(6)
C(31)	0.397(1)	0.562(1)	0.4705(7)	0.061(9)
O(31)	0.3901(8)	0.4947(7)	0.4894(5)	0.086(7)
C(32)	0.499(1)	0.685(1)	0.4876(6)	0.058(8)
O(32)	0.5607(7)	0.7009(8)	0.5150(5)	0.084(6)
C(41)	0.526(1)	0.797(1)	0.3784(6)	0.045(7)
O(41)	0.5862(7)	0.8162(8)	0.3959(5)	0.080(6)
C(42)	0.425(1)	0.770(1)	0.2707(6)	0.050(8)
O(42)	0.4246(7)	0.7691(8)	0.2218(4)	0.071(6)
C(51)	0.108(1)	0.592(1)	0.3146(8)	0.071(9)
O(51)	0.0831(9)	0.5285(8)	0.3195(7)	0.123(9)
C(52)	0.1273(9)	0.692(1)	0.2282(7)	0.050(7)
O(52)	0.1078(8)	0.6894(8)	0.1781(5)	0.088(7)
C(53)	0.075(1)	0.758(1)	0.3142(7)	0.072(9)
O(53)	0.0239(7)	0.8004(8)	0.3180(6)	0.097(7)
C(61)	0.210(1)	0.620(1)	0.4454(8)	0.07(1)
O(61)	0.1859(7)	0.5568(7)	0.4583(6)	0.090(7)
C(62)	0.171(1)	0.7843(9)	0.4374(6)	0.043(7)
O(62)	0.1232(8)	0.8268(8)	0.4482(5)	0.088(7)
C(71)	0.327(1)	0.638(1)	0.5655(7)	0.068(9)
O(71)	0.3230(9)	0.5751(8)	0.5880(5)	0.115(9)
C(72)	0.269(1)	0.788(1)	0.5638(7)	0.07(1)
O(72)	0.2200(8)	0.8217(9)	0.5813(5)	0.099(7)
C(73)	0.424(1)	0.766(1)	0.5843(7)	0.065(9)
O(73)	0.4773(8)	0.7893(9)	0.6178(5)	0.093(7)
C(81)	0.456(1)	0.882(1)	0.4812(7)	0.060(9)
O(81)	0.5183(7)	0.9021(8)	0.5035(5)	0.079(6)
C(82)	0.310(1)	0.941(1)	0.4471(8)	0.07(1)
O(82)	0.2719(9)	0.9976(9)	0.4535(6)	0.124(9)
C(91)	0.473(1)	0.982(1)	0.3711(7)	0.064(9)
O(91)	0.5305(8)	1.0128(7)	0.3912(5)	0.080(7)
C(92)	0.325(1)	1.036(1)	0.3435(8)	0.07(1)
O(92)	0.2924(9)	1.0973(9)	0.3430(7)	0.14(1)
C(93)	0.384(1)	0.955(1)	0.2672(7)	0.056(8)
O(93)	0.3917(7)	0.9642(8)	0.2187(5)	0.083(7)
C(101)	0.2556(9)	0.8237(9)	0.2458(6)	0.040(7)
O(101)	0.2479(7)	0.8290(7)	0.1959(4)	0.057(5)
C(102)	0.193(1)	0.899(1)	0.3254(6)	0.053(8)
O(102)	0.1472(7)	0.9496(8)	0.3292(6)	0.087(7)
C(111)	0.932(1)	0.6640(9)	0.3929(7)	0.057(9)
O(111)	0.9901(8)	0.6420(9)	0.4162(5)	0.095(7)

Table 2 (continued)

Atom	x	y	z	U_{eq} (Å^2)
C(112)	0.802(1)	0.590(1)	0.3439(7)	0.057(8)
O(112)	0.7796(8)	0.5200(7)	0.3363(6)	0.096(8)
C(121)	0.839(1)	0.946(1)	0.3377(6)	0.046(7)
O(121)	0.8618(8)	0.9876(7)	0.3059(5)	0.084(7)
C(122)	0.743(1)	0.9545(9)	0.4054(7)	0.051(8)
O(122)	0.7000(7)	1.0050(7)	0.4122(5)	0.078(7)
C	0.3331(9)	0.7429(9)	0.3852(6)	0.028(6)
N(1)	0.8972(7)	0.9017(8)	0.4671(5)	0.043(6)
C(2)	0.957(1)	0.852(1)	0.4852(7)	0.066(9)
C(3)	1.011(1)	0.857(1)	0.5366(7)	0.073(9)
C(4)	1.003(1)	0.919(1)	0.5732(7)	0.066(9)
C(5)	0.942(1)	0.974(1)	0.5569(7)	0.07(1)
C(6)	0.894(1)	0.963(1)	0.5038(6)	0.054(8)
N(1′)	0.8620(7)	0.7084(8)	0.2699(5)	0.047(6)
C(2′)	0.896(1)	0.643(1)	0.2488(7)	0.052(8)
C(3′)	0.913(1)	0.649(1)	0.1959(7)	0.067(9)
C(4′)	0.899(1)	0.718(1)	0.1630(8)	0.10(1)
C(5′)	0.862(1)	0.785(1)	0.1810(7)	0.08(1)
C(6′)	0.845(1)	0.777(1)	0.2348(7)	0.058(8)
N(01)	0.7775(7)	0.7819(8)	0.4436(4)	0.040(5)
C(02)	0.7980(9)	0.7036(9)	0.4318(6)	0.043(7)
C(03)	0.793(1)	0.640(1)	0.4725(7)	0.060(8)
C(04)	0.763(1)	0.658(1)	0.5194(7)	0.060(8)
C(05)	0.741(1)	0.737(1)	0.5277(6)	0.067(9)
C(06)	0.749(1)	0.796(1)	0.4900(6)	0.052(8)
N(01′)	0.7269(7)	0.7488(8)	0.3129(5)	0.046(6)
C(02′)	0.7216(9)	0.8325(9)	0.3235(6)	0.039(7)
C(03′)	0.6598(9)	0.875(1)	0.2905(6)	0.048(7)
C(04′)	0.606(1)	0.832(1)	0.2493(7)	0.069(9)
C(05′)	0.612(1)	0.752(1)	0.2400(7)	0.08(1)
C(06′)	0.673(1)	0.709(1)	0.2727(6)	0.054(8)
Cl(1) [a]	−0.0307(9)	0.888(1)	0.0704(6)	0.26(1)
Cl(2) [a]	0.0865(9)	0.903(1)	0.0623(6)	0.38(2)
Cl(3) [a]	0.0582(6)	0.9086(7)	0.1731(5)	0.157(7)
C(0)	0.0360(9)	0.8665(9)	0.0958(6)	0.44(5)

[a] Site occupancy factors: Cl(1) 0.556(9), Cl(2) 0.800(9), Cl(3) 0.64(1).

hole [9] and (iii) the solid-state packing of this M_{10} "giant tetrahedral" anion with an unusual cation (packing of such anions with more conventional counterions (e.g. $[PPN]^+$) has been of interest recently) [12,13].

2.2. X-ray structure of $[Ru_2(\mu\text{-}H)(\mu\text{-}NC_5H_4)_2(CO)_4(NC_5H_5)_2][Ru_{10}(\mu\text{-}H)(\mu_6\text{-}C)(CO)_{24}]$ (1a)

ORTEP plots of the cation (a) and anion (b) are shown in Fig. 1, a cell-packing diagram is given in Fig. 2, a summary of crystal and refinement data is presented in Table 1, fractional coordinates are listed in Table 2 and selected bond lengths and angles are displayed in Table 3. (Supplementary data were deposited earlier [10].)

The X-ray structural determination confirms the presence of the bimetallic cation and decametallic anion. The cation has two bridging pyridyls in a head-to-tail arrangement, a bridging hydrido (located in the structural determination), two σ-bound pyridines and four terminal carbonyls. The Ru–Ru bond (2.963(2) Å) is typical for Ru–Ru linkages bearing bridging hydrides and bridging imino or pyridyl groups [2]. We have previously noted that located hydrido ligands in complexes of this type are rare [2]; in the present case, errors associated with distances involving the bridging hydride (Ru(11)–H 1.8(1) Å, Ru(12)–H 1.6(1) Å) are large, and comments involving its disposition (symmetric or otherwise) are not warranted. There are two carbonyl ligands per ruthenium; those *trans* to the hydride (Ru(11)–C(112) 1.82(2) Å, Ru(12)–C(122) 1.84(2) Å) involve bonding interactions perhaps shorter than those *trans* to the pyridyl-*N* (Ru(11)–C(111) 1.90(2) Å, Ru(12)–C(121) 1.87(2) Å) with all four carbonyl ligands essentially linear (∠176(2)–178(2)°). The bridging pyridyls are arranged head-to-tail; although the anisotropy and disposition of the Ru-bound *C* and *N* are less agreeable than those of the other pyridyl and pyridine atoms, and the possibility of some disorder cannot be ruled out, the arrangement as found is consistent with the single isomer found in the ^{1}H

NMR spectrum. The Ru–C (2.06(2), 2.04(1) Å) and Ru–N (2.11(1), 2.10(1) Å) distances are unexceptional, as are the intra-ligand distances in the pyridyl and pyridine groups. Ru–N distances for the σ-bound pyridines (2.22(1), 2.20(1) Å) are long, but consistent with those in ruthenium clusters containing σ-bound pyridines which we structurally characterized previously [3].

The anion has ten ruthenium atoms arranged as a tetra-capped octahedron, with a carbide ligand occupy-

Table 3
Selected bond lengths (Å) and angles (°) for **1a**

Anion bond lengths (Å)			
External Ru–Ru bonds			
Ru(1)–Ru(2)	2.778(2)	Ru(1)–Ru(3)	2.791(2)
Ru(1)–Ru(4)	2.764(2)	Ru(2)–Ru(5)	2.782(2)
Ru(3)–Ru(7)	2.791(2)	Ru(4)–Ru(9)	2.759(2)
Ru(5)–Ru(6)	2.783(2)	Ru(5)–Ru(10)	2.759(2)
Ru(6)–Ru(7)	2.764(2)	Ru(7)–Ru(8)	2.877(2)
Ru(8)–Ru(9)	2.823(2)	Ru(9)–Ru(10)	2.748(2)
Internal Ru–Ru bonds			
Ru(2)–Ru(3)	2.854(2)	Ru(2)–Ru(4)	2.858(2)
Ru(2)–Ru(6)	2.855(2)	Ru(2)–Ru(10)	2.864(2)
Ru(3)–Ru(4)	2.843(2)	Ru(3)–Ru(6)	2.875(2)
Ru(3)–Ru(8)	2.848(2)	Ru(4)–Ru(8)	2.846(2)
Ru(4)–Ru(10)	2.834(2)	Ru(6)–Ru(8)	2.878(2)
Ru(6)–Ru(10)	2.853(2)	Ru(8)–Ru(10)	2.864(2)
Ru–carbide bonds			
Ru(2)–C	2.03(1)	Ru(3)–C	2.00(1)
Ru(4)–C	2.03(2)	Ru(6)–C	2.00(1)
Ru(8)–C	2.02(1)	Ru(10)–C	2.03(1)
Cation bond lengths (Å)			
Ru(11)–Ru(12)	2.963(2)		
Ru(11)–N(01′)	2.11(1)	Ru(12)–N(01)	2.10(1)
Ru(11)–C(02)	2.06(2)	Ru(12)–C(02′)	2.04(1)
Ru(11)–N(1′)	2.22(1)	Ru(12)–N(1)	2.20(1)
N(01′)–C(02′)	1.36(2)	N(01)–C(02)	1.35(2)
Ru(11)–H	1.8(1)	Ru(12)–H	1.6(1)
Anion bond angles (°)			
Ru(1)–Ru(2)–Ru(5)	176.58(7)	Ru(1)–Ru(3)–Ru(7)	176.85(7)
Ru(5)–Ru(6)–Ru(7)	178.05(9)	Ru(1)–Ru(4)–Ru(9)	178.23(8)
Ru(5)–Ru(10)–Ru(9)	178.52(8)	Ru(7)–Ru(8)–Ru(9)	174.42(6)
Ru(2)–Ru(1)–C(11)	105.8(6)	Ru(2)–Ru(1)–C(13)	96.8(6)
Ru(3)–Ru(1)–C(11)	101.5(6)	Ru(3)–Ru(1)–C(12)	105.5(6)
Ru(4)–Ru(1)–C(12)	98.4(5)	Ru(4)–Ru(1)–C(13)	100.1(5)
Ru(1)–Ru(2)–C(21)	91.3(6)	Ru(1)–Ru(2)–C(22)	91.9(5)
Ru(5)–Ru(2)–C(21)	92.1(6)	Ru(5)–Ru(2)–C(22)	88.5(5)
Ru(1)–Ru(3)–C(31)	87.3(6)	Ru(1)–Ru(3)–C(32)	90.4(6)
Ru(7)–Ru(3)–C(31)	92.1(6)	Ru(7)–Ru(3)–C(32)	92.7(6)
Ru(1)–Ru(4)–C(41)	89.3(5)	Ru(1)–Ru(4)–C(42)	89.1(5)
Ru(9)–Ru(4)–C(41)	92.4(5)	Ru(9)–Ru(4)–C(42)	90.2(5)
Ru(2)–Ru(5)–C(51)	100.5(6)	Ru(2)–Ru(5)–C(52)	102.6(5)
Ru(6)–Ru(5)–C(51)	102.6(5)	Ru(6)–Ru(5)–C(53)	98.8(5)
Ru(10)–Ru(5)–C(52)	100.3(5)	Ru(10)–Ru(5)–C(53)	99.3(6)
Ru(5)–Ru(6)–C(61)	91.9(5)	Ru(5)–Ru(6)–C(62)	89.9(4)
Ru(7)–Ru(6)–C(61)	87.8(5)	Ru(7)–Ru(6)–C(62)	92.1(4)
Ru(3)–Ru(7)–C(71)	97.3(6)	Ru(3)–Ru(7)–C(73)	100.3(6)
Ru(6)–Ru(7)–C(71)	103.7(5)	Ru(6)–Ru(7)–C(72)	98.2(5)
Ru(8)–Ru(7)–C(72)	108.3(6)	Ru(8)–Ru(7)–C(73)	97.4(6)
Ru(7)–Ru(8)–C(81)	93.5(5)	Ru(7)–Ru(8)–C(82)	103.3(6)
Ru(9)–Ru(8)–C(81)	91.1(5)	Ru(9)–Ru(8)–C(82)	79.4(6)
Ru(4)–Ru(9)–C(91)	97.8(5)	Ru(4)–Ru(9)–C(93)	98.6(6)
Ru(8)–Ru(9)–C(91)	98.6(5)	Ru(8)–Ru(9)–C(92)	104.8(6)
Ru(10)–Ru(9)–C(92)	102.7(6)	Ru(10)–Ru(9)–C(93)	101.6(5)
Ru(5)–Ru(10)–C(101)	90.0(5)	Ru(5)–Ru(10)–C(102)	90.2(5)
Ru(9)–Ru(10)–C(101)	89.4(5)	Ru(9)–Ru(10)–C(102)	91.2(5)

ing the central cavity. The 24 terminal carbonyl ligands are arranged three per apical ruthenium and two per edge ruthenium; all Ru–C–O angles are approximately linear (∠173(2)–180(1)°) with no evidence of semi-bridging interactions. It was surprising that no residues representing substantial hydride fractions were evident about the anion (particular examination being made of the region between Ru(7) and Ru(8) where the carbonyl groups are substantially splayed), given that the cation "organic" hydrogen atoms were located in difference maps and constrained, and that the hydride bridging the two Ru atoms in the cation was clearly evident and refined in (x, y, z). Crystallographic evidence for the anionic hydride is therefore circumstantial, although this indirect evidence for its location, which follows, is strong.

The Ru–Ru distances fall neatly into two bands: those for the central octahedral unit (2.834(2)–2.875(2) Å, average 2.86 Å) and those involving the apical rutheniums (but excluding Ru(7)–Ru(8) 2.877(2) Å and Ru(8)–Ru(9) 2.823(2) Å)) (2.748(2)–2.791(2) Å, average 2.77 Å). Such a differentiation between central core and apical distances has been observed in previous structural determinations of "giant tetrahedral" cores. In this context, the unusual distances along Ru(7)–Ru(8)–Ru(9) are strongly indicative of the presence of an edge-bridging hydride. Angles about the "giant tetrahedron" are also consistent with an unusual Ru(7)–Ru(8)–Ru(9) vector. Angle sums (∠CO–Ru(a)–Ru(b) + ∠Ru(a)–Ru(b)–CO) for cisoid carbonyls are 187.7–197.1° except ∠C(72)–Ru(7)–Ru(8) + ∠Ru(7)–Ru(8)–C(82) (211.6°) and ∠C(82)–Ru(8)–Ru(9) + ∠Ru(8)–Ru(9)–C(92) (184.2°). The hydrido ligand, as postulated on Ru(7)–Ru(8) between C(72) and C(82), is consistent with a lengthening of the metal–metal bond, a "splaying back" of CO(72) and CO(82) and a concomitant "folding in" of CO(82) and CO(92); this "folding in" is probably responsible for the slight lengthening of Ru(8)–Ru(9). The (hydrido)decametallic cluster anions have been suggested as model systems for the chemisorption of synthesis gas on the surface of bulk metals or colloidal particles [14], owing to the "close-packed" arrays of carbonyl ligands approximately perpendicular to the surface found in previous structural determinations; this is the first example from this system showing the marked displacement of carbonyl ligands normally found with edge-bridging hydrides in low nuclearity clusters.

Ruthenium clusters with hydrido ligands in octahedral interstitial sites are well known (e.g. $[Ru_6(\mu_6\text{-}H)(CO)_{18}]^-$ [15,16] and $[Ru_8(\mu\text{-}H)(\mu_6\text{-}H)(CO)_{21}]^{2-}$ [17]). No structurally characterized example of a tetrahedral interstitial hydrido ligand has thus far been established. Based on spectroscopic data [18] and structural determinations of the $[AsPh_4]^+$ and $[PMePh_3]^+$ salts [19], it was proposed some time ago that $[HOs_{10}C(CO)_{24}]^-$ contains a hydrido ligand in a tetrahedral site. However, a neutron diffraction study on the related cluster $[H_4Os_{10}(CO)_{24}]^{2-}$ revealed that the four hydrido ligands were external to the cluster core [14], and recent spectroscopic studies have cast doubts on the interstitial location of the hydrido in $[HOs_{10}C(CO)_{24}]^-$ [20]. The present work probably eliminates the $[HM_{10}C(CO)_{24}]^-$ system as candidates for clusters containing hydrido ligands in tetrahedral holes.

Braga and co-workers have discussed solid-state interactions of the "giant tetrahedral" clusters $H_2Os_{10}C(CO)_{24}$ [13], $[Os_{10}C(CO)_{24}]^{2-}$, $[Os_{10}C(CO)_{22}(NO)(I)]^{2-}$, $[H_4Os_{10}(CO)_{24}]^{2-}$, $[Ru_{10}C(CO)_{24}]^{2-}$ (all as $[PPN]^+$ salts) and $[HOs_{10}C(CO)_{24}]^-$ (as $[PMePh_3]^+$ and $[AsPh_4]^+$ salts) [12]. The salts in particular are relevant to the present investigation, packing as "anion piles surrounded by cation belts". The $[Ru_{10}(\mu\text{-}H)(\mu_6\text{-}C)(CO)_{24}]^-$ anions in the present salt exhibit the same packing motif as the previously structurally characterized $[HOs_{10}C(CO)_{24}]^-$, being "apex-to-base" linked along the c axis of the cell, via the interaction of one tricarbonyl unit of one anion with the triangular face of a neighbouring anion. There is also some mutual CO · · · CO penetration of adjacent anion piles to maximize favourable C · · · O interactions. Although Braga and co-workers were able to show that $[Ru_{10}C(CO)_{24}]^{2-}$ packs similarly to $[Os_{10}C(CO)_{24}]^{2-}$ and related decaosmium dianions ("edge-to-edge"), and that decaosmium monoanions adopt a different packing geometry, this is the first evidence for the decaruthenium anion behaving in the same manner as the decaosmium anion and different to the decaruthenium dianion; such a result is perhaps not surprising, given the similar size and identical charge.

2.3. Reactivity of $[Ru_2(\mu\text{-}H)(\mu\text{-}NC_5H_4)_2(CO)_4(NC_5H_5)_2][Ru_{10}(\mu\text{-}H)(\mu_6\text{-}C)(CO)_{24}]$ (1a) and $[PPh_4][Ru_{10}(\mu\text{-}H)(\mu_6\text{-}C)(CO)_{24}]$ (1b) toward triphenylphosphine

The chemistry of the "giant tetrahedral" cluster $[Os_{10}(\mu_6\text{-}C)(CO)_{24}]^{2-}$ has been reported in depth [21–24]; a range of electrophiles can be added, but the cluster is reported to have a "remarkable resistance to ... nucleophiles" [24], requiring Os–Os cleavage by halogens and harsh reaction conditions. In sharp contrast, nucleophilic substitution of $[Ru_{10}(\mu\text{-}H)(\mu_6\text{-}C)(CO)_{24}]^-$ by PPh_3 occurs in a stepwise manner under exceptionally mild conditions to afford (hydrido)-(carbido)decaruthenium cluster anions containing from one to four phosphine ligands [1]. Thus, addition of an approximately equimolar amount of triphenylphosphine to $[Ru_2(\mu\text{-}H)(\mu\text{-}NC_5H_4)_2(CO)_4(NC_5H_5)_2][Ru_{10}(\mu\text{-}H)(\mu_6\text{-}C)(CO)_{24}]$ (**1a**) at room temperature resulted in an immediate change in the IR spectrum. Crystallization from CH_2Cl_2 afforded green–black nee-

Table 4
Spectroscopic data for the decaruthenium cluster anions

Compound	^{1}H NMR hydride resonance (ppm)	^{13}C NMR carbide resonance (ppm)	^{31}P NMR (ppm)	Negative ion FAB-MS (m/z)	IR, ν(CO) (cm^{-1})
1a	−13.55	374.6	–	1696	2053s, 2009s, 1994m (sh)
2a	−11.54	378.8	44.4	1930	2077w, 2047s, 2016m, 2000m
3a	−11.50	381.5	52.1, 43.0 (1 : 1)	2165	2064m, 2041s, 2011s (sh), 2006s, 1990s
4a	−11.58	384.0	50.0, 41.9 (2 : 1)	2399	2049m, 2013s, 2000vs, 1985m (sh)
5c	−11.54	386.6	48.0, 40.5 (3 : 1)	2633	2024w, 1996s, 1972m (sh)

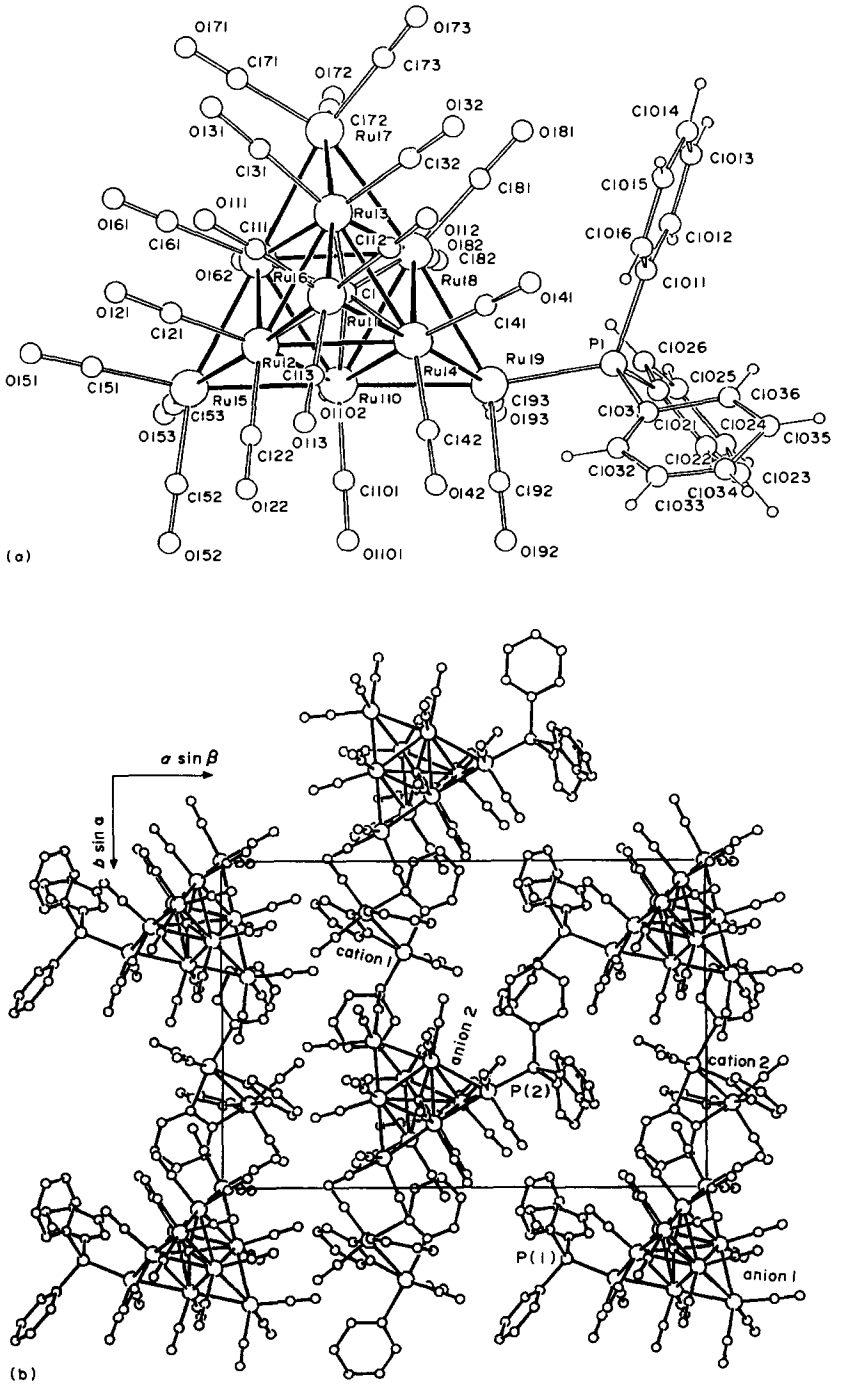

Fig. 3. (a) ORTEP plot of the anion geometry in $[Ru_2(\mu\text{-H})(\mu\text{-NC}_5H_4)_2(CO)_4(NC_5H_5)_2][Ru_{10}(\mu\text{-H})(\mu_6\text{-C})(CO)_{23}(PPh_3)]$ (**2a**). 20% thermal envelopes are shown for the non-hydrogen atoms. Hydrogen atoms have arbitrary radii of 0.1 Å. (b) Unit cell of **2a** (triclinic, $P1$ (quasi-$P\bar{1}$), $a = 21.625(5)$, $b = 14.80(1)$, $c = 12.387(4)$ Å, $\alpha = 81.73(4)$, $\beta = 80.07(2)$, $\gamma = 88.53(4)°$, $Z = 2$).

dles of $[Ru_2(\mu\text{-}H)(\mu\text{-}NC_5H_4)_2(CO)_4(NC_5H_5)_2]$-$[Ru_{10}(\mu\text{-}H)(\mu_6\text{-}C)(CO)_{23}(PPh_3)]$ (**2a**) in high yield. Similarly, addition of 2–4 equiv. of PPh_3 to **1a** at room temperature afforded the bis- and trisphosphine-substituted decaruthenium complexes, $[Ru_2(\mu\text{-}H)(\mu\text{-}NC_5H_4)_2(CO)_4(NC_5H_5)_2][Ru_{10}(\mu\text{-}H)(\mu_6\text{-}C)(CO)_{22}(PPh_3)_2]$ (**3a**) and $[Ru_2(\mu\text{-}H)(\mu\text{-}NC_5H_4)_2(CO)_4(NC_5H_5)_2][Ru_{10}(\mu\text{-}H)(\mu_6\text{-}C)(CO)_{21}(PPh_3)_3]$ (**4a**), respectively. Formation of the tetrakis-substituted cluster anion, $[Ru_{10}(\mu\text{-}H)(\mu_6\text{-}C)(CO)_{20}(PPh_3)_4]^-$ (**5c**), as its $[Ru_2(\mu\text{-}H)(\mu\text{-}NC_5H_4)_2(CO)_4(PPh_3)_2]^+$ salt required a 12-fold excess of ligand and reaction in refluxing acetone for 2 h. Clusters **2a–4a** and **5c** were characterized by a combination of solution IR, ^1H, ^{13}C and ^{31}P NMR spectroscopy, FAB-MS and, in the case of **2a**, by a single-crystal X-ray study; important spectroscopic data are summarized in Table 4. Other spectroscopic data have been reported elsewhere [1].

The chemical shift of the hydride resonance in the ^1H NMR spectrum is relatively insensitive to events beyond the immediate tetrahedral cap at which it resides; thus, substitution of **1a** to **2a** involves a downfield shift of 2 ppm (and conversion from singlet to doublet), but subsequent substitution at the other caps to afford successively **3a**, **4a** and **5c** has little effect on its chemical shift. In **2a–4a** and **5c**, the coupling of this hydride (J(HP) 7 Hz) is consistent with *cis*-disposed ligation of hydride and phosphine. There is a fairly constant downfield march of the carbide resonance in the ^{13}C NMR spectrum on consecutive substitution, corresponding to about 2.5 ppm per phosphine; clearly, the interstitial location and relative remoteness (three bonds from phosphorus) do not prevent its being influenced by apical cluster substitution. The ^{31}P NMR spectra are particularly informative; *P*-substitution at the hydride-containing apex gives a resonance at 44.4 ppm, which shifts 1–1.5 ppm upfield for each successive phosphine substitution at the other apices in **3a**, **4a** and **5c**. The non-hydride-apical phosphine appears at 52.1 ppm in **3a**, and moves about 2 ppm upfield for each subsequent substitution in **4a** and **5c**. The FAB mass spectra contain signals in both positive and negative ion spectra for the cations and anions of these salts, respectively. The negative ion FAB mass spectrum of **4a** contains a peak due to $[M - PPh_3 + CO]$; this parallels its stability in solution where ^{31}P and ^{13}C NMR spectroscopy revealed slow conversion to **3a**, the PPh_3 conceivably being replaced by CO scavenged from slight decomposition of the cluster anion or cation. However, attempted conversion of **4a** to **3a** by refluxing **4a** in CH_2Cl_2 for 6 h failed to reveal evidence for the formation of the **3a**.

An interesting observation for this series of complexes is that substitution at the "giant tetrahedral" cluster anion is so facile that it occurs before replacement of the σ-bound pyridines of the cluster cation; although σ-pyridine often has a "lightly stabilizing" role in polynuclear chemistry [3], in these clusters it is displaced less readily than the apical carbonyls on the anion.

The structure of **2a** has been reported previously [1]; the ORTEP plot showing the anion geometry is shown in Fig. 3(a). The metal framework has a tetra-capped octahedral geometry, and interstitial carbide sitting in the octahedral cavity, as in the precursor **1a**. The structural study confirms substitution of an apical carbonyl by the triphenylphosphine, but the imprecision of the structural determination does not permit confirmation of the spectroscopically assigned hydride ligand site. Fig. 3(b) shows the unit cell of **2a**. It is clear that the "anion piles" and other unique packing characteristics of the precursor **1a** (see Fig. 2) have been disrupted by the introduction of PPh_3; maintaining the packing geometry of the precursor would presumably require the introduction of a ligand isosteric with CO (as observed, for example, in $[Os_{10}C(CO)_{22}(NO)(I)]^{2-}$ [12].

2.4. Comments on the diruthenium cations and metathetical procedures

The $[Ru_2(\mu\text{-}H)(\mu\text{-}NC_5H_4)_2(CO)_4(NC_5H_5)_2]^+$ cation formed in the synthesis of **1a** is not an innocent spectator ion. It is unstable to preparative thin-layer chromatography, causing problems with product purification; we have been unable to identify the resultant species, although loss of the hydride is observed by ^1H NMR. It was also found to compete, to a minor extent, with the anion for phosphine substitution on prolonged stirring (over a period of several hours) with fourfold PPh_3 or greater, as evidenced by the occurrence of a doublet (-11.96 ppm, J(HP) 15 Hz, 5–15%) presumably due to $[Ru_2(\mu\text{-}H)(\mu\text{-}NC_5H_4)_2(CO)_4(NC_5H_5)(PPh_3)]^+$. As mentioned above, the synthesis of the tetrakis-PPh_3 cluster anion (**5c**), which requires a large excess of PPh_3 and more forcing conditions, gives a PPh_3-disubstituted cation, identified by the triplet hydride signal in the ^1H NMR spectrum (-12.65 ppm, J(HP) 11 Hz) and a new signal in the ^{31}P NMR spectrum (26.6 ppm) [1]. Additionally, extended stirring of a reaction mixture seems to promote a small amount of conversion of the head-to-tail isomer (^1H NMR hydride signal at -10.75 ppm) to the head-to-head arrangement (hydride signal at -10.35 ppm), similar to those obtained by Cockerton and Deeming [11] in the $Ru_2(\mu\text{-}NC_5H_4)_2(CO)_6$ system.

In view of some of the above problems, replacement of the diruthenium cation was pursued. Stirring a mixture of **1a** and [PPN]Cl in acetone for 20 min achieved complete deprotonation of the cluster anion, affording $[PPN]_2[Ru_{10}(\mu_6\text{-}C)(CO)_{24}]$ in good yield. We were unable to protonate this dianion effectively as a route into the PPN^+ salt of $[Ru_{10}(\mu\text{-}H)(\mu_6\text{-}C)(CO)_{24}]^-$; addition of HBF_4, HCl or DMA · HPF_6 to acetone solutions of

$[PPN]_2[Ru_{10}(\mu_6\text{-}C)(CO)_{24}]$ afforded only trace amounts of the desired product or decomposition of the cluster to an unidentified insoluble material. Attempted metathesis of **1a** using other quaternary alkyl- or arylammonium halides, $[PF_6]^-$ or $[BF_4]^-$ salts gave mixtures of the protonated and deprotonated anions together with partial metathesis of the cation. Successful metathesis was obtained by adding the stoichiometric amount of $[PPh_4][BF_4]$ to the triruthenium precursor $Ru_3(\mu\text{-}H)(\mu\text{-}NC_5H_4)(CO)_{10}$ and refluxing the mixture in chlorobenzene as above. The desired product $[PPh_4][Ru_{10}(\mu\text{-}H)(\mu_6\text{-}C)(CO)_{24}]$ (**1b**) was obtained in around 45% yield, together with the deprotonated cluster $[PPh_4]_2[Ru_{10}(\mu_6\text{-}C)(CO)_{24}]$ and some $[PPh_4][Ru_6(\mu_6\text{-}H)(CO)_{18}]$.

Analogous triphenylphosphine-substituted clusters can be prepared as their $[PPh_4]^+$ salts in comparable yields by employing **1b** as the precursor. Although $[PPh_4][Ru_6(\mu_6\text{-}H)(CO)_{18}]$ is difficult to separate from **1b** by thin-layer chromatography, having a similar R_f, the phosphine-substituted derivatives are easily purified. Analytical and spectroscopic data of the precursor and the phosphine-containing derivatives are contained in the Experimental section; there are no substantive differences in anion spectral data from the analogous complexes as $[Ru_2(\mu\text{-}H)(\mu\text{-}NC_5H_4)_2(CO)_4(NC_5H_5)_2]^+$ salts.

2.4. Fluxionality studies

Some reactions catalysed by metal particles require that chemisorbed species such as H and CO are mobile on the metal surface and, if the cluster–surface analogy holds, information about this mobility can be gained from the dynamic behaviour of similar ligands coordinated to metal clusters. Bailey et al. [20] have previously reported studies of carbonyl and, particularly, hydride ligand site exchange in $[HM_{10}C(CO)_{24}]^-$ (M = Ru, Os). We examined the carbonyl and hydride ligand fluxionality on clusters **1a–4a** and **5c** using $^{13}C\text{-}\{^1H\}$ exchange spectroscopy (EXSY). These experiments use a NOESY sequence which allows for a "mixing time" during which the observed nuclei may migrate to another site. Assuming there are no direct $^{13}C\text{–}^{13}C$ dipolar interactions, the off-diagonal cross-peaks in the 2D experiment occur between the shifts of exchanging sites [25]. Fig. 4 shows the carbonyl ligand labelling scheme used in the fluxionality discussions; $^{13}C\text{-}\{^1H\}$ EXSY contour plots for clusters **2a–4a** and **5c** are shown in Figs. 5–9 below.

Variable-temperature ^{13}C NMR spectra for $[Ru_{10}(\mu\text{-}H)(\mu_6\text{-}C)(CO)_{24}]^-$ over the range 250–380 K have been reported by Bailey et al. and are consistent with the following: (i) at the lowest temperature, rapid migration of the hydride around the symmetry-related edges and faces of a single capping tetrahedron of the Ru_{10} core, possibly synchronous with $Ru(CO)_3$ "rotation"; (ii) at higher temperatures, total fluxionality of the hydride over the surface of the metal core; and (iii) at the highest temperature, slow CO migration between metal atoms.

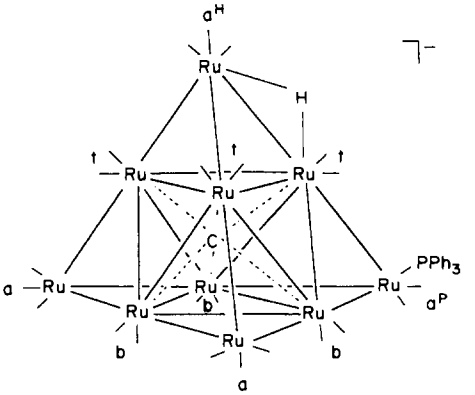

Fig. 4. CO labelling scheme for fluxionality studies. a = apical; a^H = apical with hydride; a^{HP} = apical with hydride and phosphine; b = basal edge; t = tetrahedral edge; c = cation; * = impurity.

The ^{13}C EXSY spectrum of **1a** at 263 K (Fig. 5(a)) is similar to that reported for $[HOs_{10}C(CO)_{24}]^-$ at 340 K, with only cross-peaks attributable to exchange between the two distinct apical $Ru(CO)_3$ sites or the three $Ru(CO)_2$–edge sites being observed; there is no exchange at this temperature between the edge and apical environments. The only explanation for these results is hydride exchange between apices (i.e. regime (ii) above). Its occurrence at a lower temperature in **1a** than in $[HOs_{10}C(CO)_{24}]^-$ confirms that such hydride migration is more facile for the cluster of the lighter metal. At 298 K (Fig. 5(b)), cross-peaks between the coalescing apical carbonyls (a and a^H) and the coalescing edge carbonyls (b and t) are observed, consistent with the onset of global exchange of the CO ligands.

The EXSY spectrum of **2a** at 298 K is shown in Fig. 6. The high-field resonance confirms rapid tripodal rotation of apical carbonyls (a) about the $Ru(CO)_3$ apices. The doublet at 200.2 ppm corresponding to the carbonyls at the $(\mu\text{-}H)Ru(CO)_2(PPh_3)$ apex (a^{HP}) has coupling consistent with *cis*-coordinated phosphine; rapid hydride scrambling about the capping tetrahedron containing the phosphine and tripodal $Ru(CO)_2(PPh_3)$ rotation is suggested by the fact that other $Ru(CO)_3$ apices are equivalent. In **1a**, exchange between a and a^H is a very facile process, and cross-peaks are observed at low temperature (Fig. 5). In **2a**, exchange between a and a^H is no longer observed. This confirms that the exchange observed for **1a** is due to the hydride mobility, the apices of **1a** being otherwise identical. Such mobility in **2a** is not sufficient, carbonyl migration being necessary. It seems likely that the hydride remains localized at the PPh_3-containing apex, although the ^{13}C EXSY spectrum cannot confirm this. As with

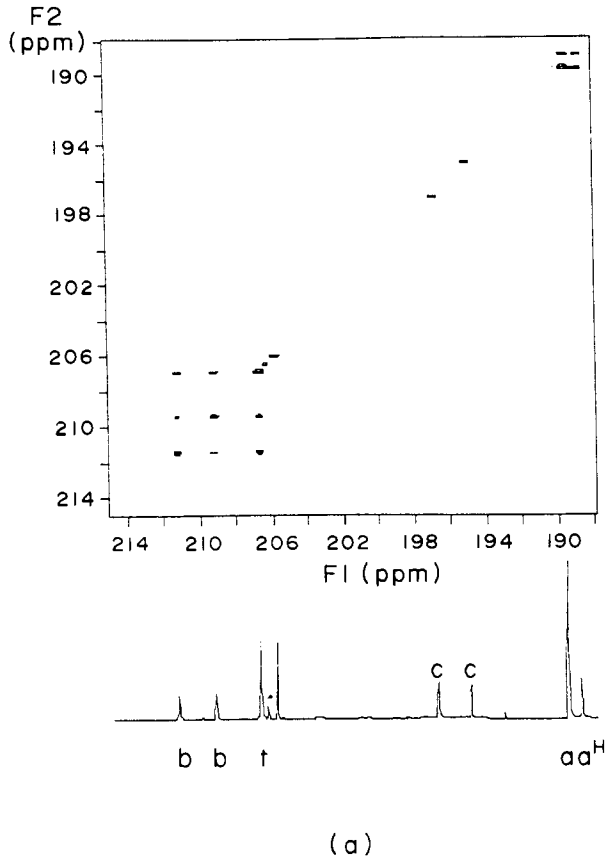

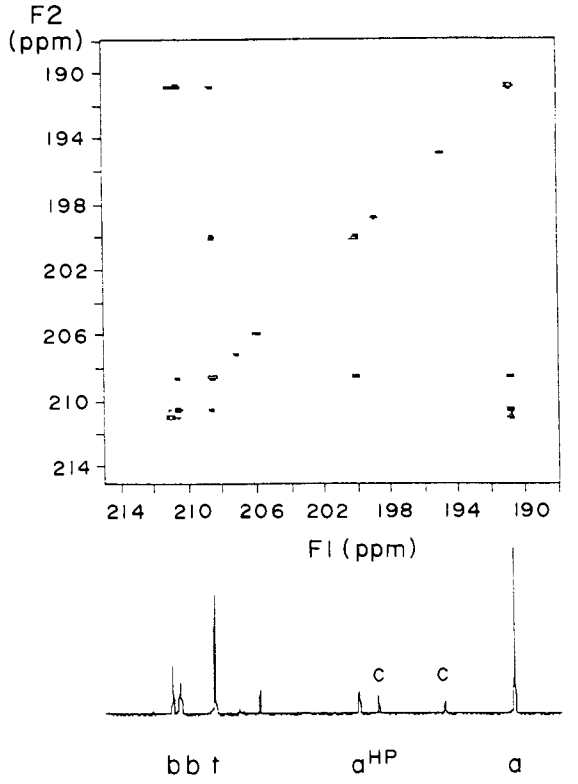

Fig. 6. ^{13}C EXSY spectrum of **2a** at 298 K.

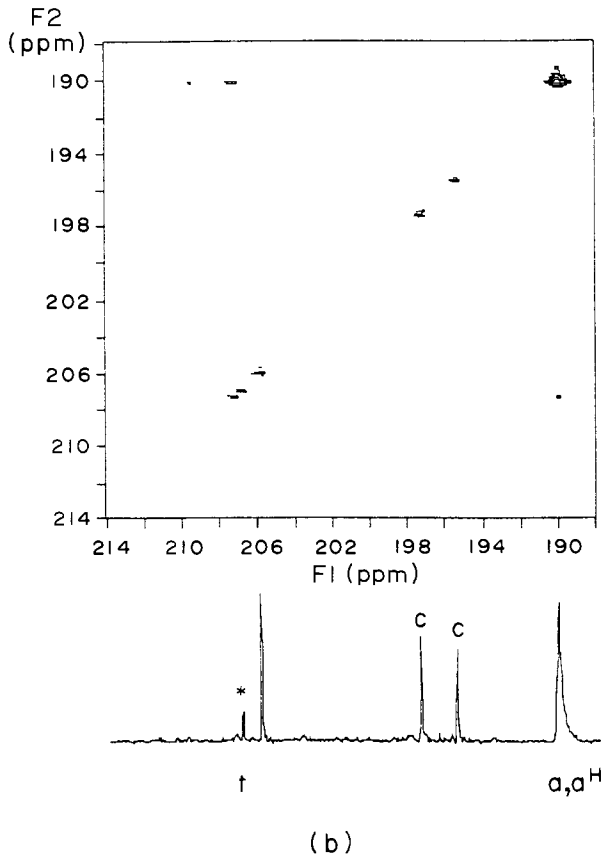

Fig. 5. ^{13}C EXSY spectra of **1a** at (a) 263 and (b) 298 K.

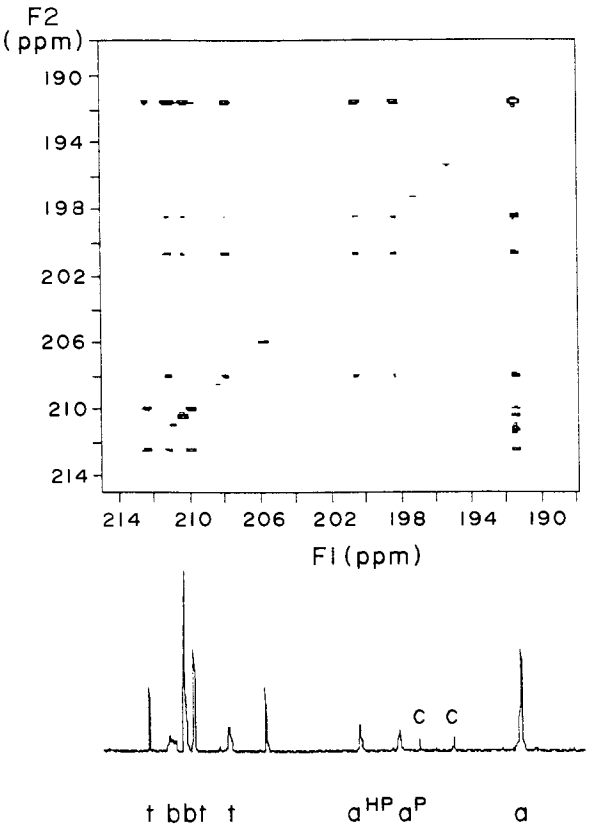

Fig. 7. ^{13}C EXSY spectrum of **3a** at 298 K.

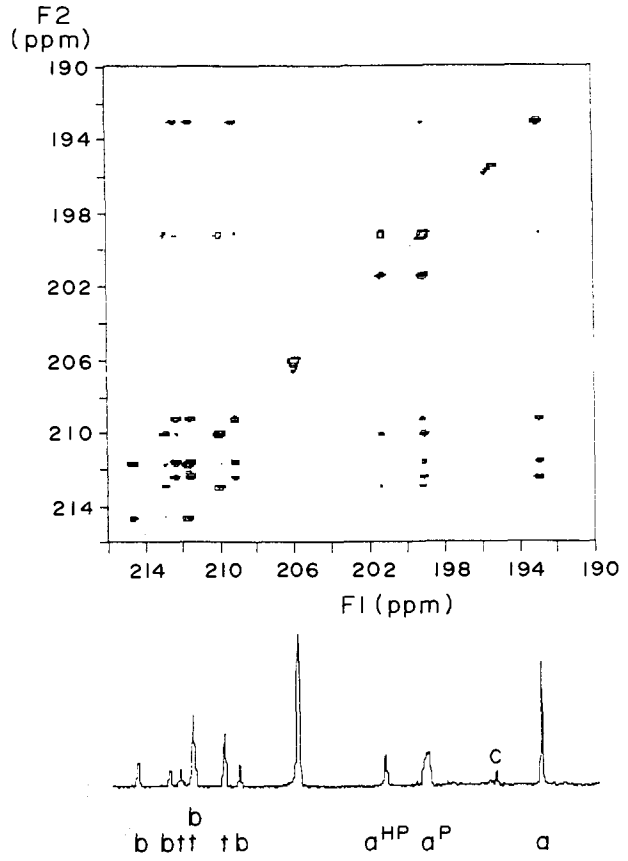

Fig. 8. ^{13}C EXSY spectrum of **4a** at 298 K.

1a, the spectrum for **2a** contains cross-peaks indicating facile exchange between basal-edge sites and basal-edge and tetrahedral sites. For **2a**, cross-peaks between the unsubstituted apices and tetrahedral or basal sites are apparent; a^{HP} only shows cross peaks with the tetrahedral edge sites, as expected.

Figs. 7 and 8 show the ^{13}C EXSY spectra at 298 K for **3a** and **4a**, respectively. Examination of Figs. 6–8 confirms that we can simultaneously observe both hydride and carbonyl fluxionality. Exchange between a^{P} and a^{HP} sites is observed for all possible cases, with particularly strong cross-peaks for **4a**; these signals must correspond to hydride mobility. There are no a^{HP} to a cross-peaks for **2a** or **4a**, but prominent signals in **3a**; these cross-peaks probe carbonyl migration, and their presence in Fig. 7, but not in Fig. 6 or 8, warrants a possible explanation. Carbonyl exchange between metals proceeds by way of bridging carbonyl intermediates which become increasingly stable as electron density at the cluster increases. Thus, in the absence of competing considerations, a fluxionality order of **1a** < **2a** < **3a** < **4a** < **5c** would be predicted. Presumably, steric problems become important with increasing substitution, so that the order **2a** < **3a** > **4a** is observed. Further inspection of Fig. 8 reveals that exchange between a^{P} and edge sites (basal or tetrahedral) is extremely facile compared with exchange between a^{HP} and the tetrahedral edge sites.

Fig. 9 shows the ^{13}C EXSY spectrum for **5c** at 298 K. It is interesting because, assuming rapid tripodal $Ru(CO)_2(PPh_3)$ rotation that the above results suggest, it should have similar effective symmetry to **1a**. The comparison between the two is therefore between related clusters of varying electron density and steric considerations. It is immediately apparent that similar cross-peaks are observed in Fig. 9 as in Fig. 5, but that exchange is more facile in the unsubstituted cluster. Whereas global exchange of carbonyl is evident in the EXSY spectrum of **1a**, that of **5c** is consistent with hydride migration between the four apices, and carbonyl exchange between all sites except those of the hydrido-containing apex.

To summarize the dynamic behaviour of the hydride and carbonyl ligands observed over this series of clusters:

(a) rapid tripodal rotation is observed about the $Ru(CO)_3$ and $Ru(CO)_2PPh_3$ apices of all the clusters;

(b) the next-lowest-energy exchange process involves adjacent COs, i.e. exchange between (i) the basal-edge sites, (ii) basal-edge and tetrahedral edge sites or (iii) apex and basal or tetrahedral sites;

(c) all polysubstituted clusters show exchange be-

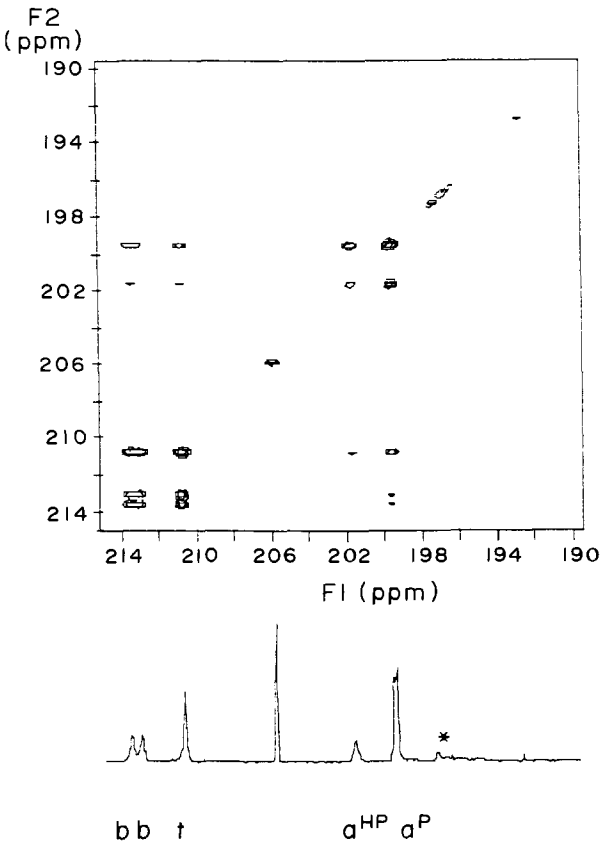

Fig. 9. ^{13}C EXSY spectrum of **5c** at 298 K.

tween the substituted apices, suggesting hydride site exchange between the phosphine-substituted caps, or centres of greatest electron density; this exchange is more facile than CO mobility for **4a** and **5c**, but less so for **3a**;

(d) in the bis-substituted cluster **3a**, additional exchange between the phosphine-substituted and unsubstituted apices suggests that complete CO scrambling is a lower energy process in this cluster than in the other members of the series. For the mono- and bis-substituted complexes, phosphine substitution decreases the energy barrier to CO fluxionality, presumably by increasing the electron density at the cluster core and thereby stabilizing intermediates bearing bridging COs. Tris-substitution presumably decreases the available CO exchange routes with respect to the less substituted clusters, increasing the energy barrier to complete CO scrambling. The tetrakis-substituted cluster **5c** is related to the unsubstituted cluster **1a** with similar, but less facile, exchange behaviour.

3. Experimental details

$Ru_3(\mu\text{-H})(\mu\text{-}NC_5H_4)(CO)_{10}$ was made as previously described [26] except that thin-layer chromatography (TLC) with light petroleum (b.p. 60–80°C) as eluent was used to resolve the product mixture. The clusters $[Ru_2(\mu\text{-H})(\mu\text{-}NC_5H_4)_2(CO)_4(NC_5H_5)_2]$-$[Ru_{10}(\mu\text{-H})(\mu_6\text{-C})(CO)_{24-x}(PPh_3)_x]$ ($x = 1$–3) and $[Ru_2(\mu\text{-H})(\mu\text{-}NC_5H_4)_2(CO)_4(PPh_3)_2][Ru_{10}(\mu\text{-H})(\mu_6\text{-C})(CO)_{20}(PPh_3)_4]$ were made by published methods [1]. Triphenylphosphine, [PPN]Cl and $HBF_4 \cdot Et_2O$ were obtained commercially and used as received. $[PPh_4][BF_4]$ was synthesized by treatment of aqueous solutions of $[PPh_4]Br$ (Strem) with $Na[BF_4]$ (BDH) (Anal. Found: C, 67.68; H, 4.82; $BC_{24}H_{20}F_4P$ Calc.: C, 67.64; H, 4.73%). DMA · HPF_6 was synthesized from dimethylamide (DMA) and HPF_6 in propionic anhydride [27]. Tetrahydrofuran (THF) was distilled from Na–benzophenone; other solvents were used as received. Reactions were carried out using Schlenk techniques [28] under dry nitrogen; subsequent work-up was carried out without any precautions to exclude air.

IR spectra were recorded using a Perkin-Elmer Model 1600 Fourier transform spectrophotometer with CaF_2 optics. NMR spectra were recorded on a Varian Gemini 300 spectrometer (^1H at 300 MHz, ^{13}C at 75 MHz and ^{31}P at 121 MHz) in acetone-d_6, unless otherwise stated. References for the ^1H and ^{13}C NMR spectra were set to residual solvent peaks; the latter were proton decoupled. The ^1H spectra for complexes containing the $[Ru_2(\mu\text{-H})(\mu\text{-}NC_5H_4)_2(CO)_4(NC_5H_5)_2]^+$ cation were obtained using a recycle delay of 20 s. The ^{31}P NMR spectra were recorded using a recycle delay of 40 s; they are reported relative to external 85% H_3PO_4 at 0.0 ppm and are proton decoupled. The ^{13}C-{^1H} EXSY experiments were carried out using the standard NOESY pulse sequence with the mixing time set to 0.200 s on samples enriched to 30–50% ^{13}CO by utilizing isotopically enriched $Ru_3(CO)_{12}$. Mass spectra were recorded using a VG ZAB 2SEQ instrument (30 kV Cs^+ ions, current 1 mA, accelerating potential 8 kV, 3-nitrobenzyl alcohol matrix) at the Australian National University; peaks were recorded as m/z. Analyses were carried out by the Microanalytical Service of the Research School of Chemistry, Australian National University. TLC was performed on glass plates (20 × 20 cm) coated with Merck GF_{254} silica gel (0.5 mm) using 1 : 1 acetone–light petroleum as eluent. Calculated yields for reactions in which **1a** is formed in situ assume complete conversion of the triruthenium precursor $Ru_3(\mu\text{-H})(\mu\text{-}NC_5H_4)(CO)_{10}$.

3.1. Synthesis of $[Ru_2(\mu\text{-H})(\mu\text{-}NC_5H_4)_2(CO)_4(NC_5H_5)_2][Ru_{10}(\mu\text{-H})(\mu_6\text{-C})(CO)_{24}]$ (1a)

A solution of $Ru_3(\mu\text{-H})(\mu\text{-}NC_5H_4)(CO)_{10}$ (167 mg, 0.252 mmol) in chlorobenzene (20 ml) was heated under reflux with vigorous stirring for 40 min. The resulting black solution was allowed to come to room temperature and filtered through a filter aid, which was washed with chlorobenzene to leave behind a small amount of black insoluble material. The combined filtrate and washings were taken to dryness in vacuo; trituration of the black residue with light petroleum (2 × 20 ml) afforded a black, microcrystalline solid identified as **1a** (119 mg, 0.0512 mmol, 81%). Anal. Found: C, 25.03; H, 1.01; N, 1.78; M^- 1704; M^+ 631. $C_{49}H_{20}N_4O_{28}Ru_{12}$ Calc.: C, 25.31; H, 0.87; N, 2.41%; M^- 1704; M^+ 631. IR (CH_2Cl_2): ν(CO) 2052s, 2009s, 1997(sh)m cm^{-1}. ^1H NMR: δ 8.61 (dt, J(HH) = 5.0 Hz, J(HH) = 1.5 Hz, 4H, H2, 2′, 6, 6′), 8.54 (dq, J(HH) = 5.0 Hz, J(HH) = 1.0 Hz, 2H, H06, 06′), 8.05 (tt, J(HH) = 7.5 Hz, J(HH) = 1.5 Hz, 2H, H4, 4′), 7.73 (dt, J(HH) = 7.5 Hz, J(HH) = 1.0 Hz, 2H, H03, 03′), 7.57 (m, J(HH) = 5.0, 7.5 Hz, J(HH) = 1.5 Hz, 4H, H3, 3′, 5, 5′), 7.52 (m, J(HH) = 7.5 Hz, J(HH) = 1.5 Hz, 2H, H04, 04′), 7.09 (m, J(HH) = 5.0, 7.5 Hz, J(HH) = 1.5 Hz, 2H, H05, 05′), −10.74 (s, 1H, Ru_2H), −13.55 (s, 1H, $Ru_{10}H$). ^{13}C NMR (298 K): δ 374.6 (μ_6-C); 190.3 ($Ru_{10}CO$; other signals for $Ru_{10}CO$ not observed); 176.3 (CO2, O2′), 155.3 (CO6, O6′), 154.9 (C2, 6, 2′, 6′), 140.9, 140.0 (CO3, O3′, C4, 4′), 136.0 (CO4, O4′), 127.1 (C3, 3′, 5, 5′), 122.4 (CO5, O5′); (263 K): δ 211.5, 209.3, 206.9, 189.7, 188.9 (ratio 3 : 3 : 6 : 9 : 3, anion CO); 197.0, 195.0 (ratio 2 : 2, cation CO). Recrystallization from acetone afforded green–black needles of **1**. Found: C, 25.82; H, 0.78; N, 1.95%.

3.2. Attempted metathesis of 1a

3.2.1. With [PPN]Cl

A solution of **1a** (19 mg, 0.0082 mmol) and [PPN]Cl (9 mg, 0.016 mmol) in acetone (15 ml) was stirred at

room temperature for 20 min. The IR and ^{1}H NMR spectra at this stage indicated complete deprotonation to the dianion $[Ru_{10}(\mu_6\text{-}C)(CO)_{24}]^{2-}$ [9] and the presence of both isomers of the diruthenium cation (hydride signals at −10.34 and −10.73 ppm). The mixture was subjected to TLC and the product from the major band crystallized from acetone to yield green–black microcrystalline $[PPN]_2[Ru_{10}(\mu_6\text{-}C)(CO)_{24}]$ (18 mg, 0.0065 mol, 79%). IR (CH_2Cl_2): ν(CO) 2025s, 2003m, 1982m cm^{-1}. ^{1}H NMR: δ 7.73–7.50 (m, PPN). ^{31}P NMR: δ 22.51 (s, PPN). ^{13}C NMR: δ 204.1 (CO); 135.7, 135.1 (d, J(CP) = 45 Hz), 130.8 (d, J(CP) = 23 Hz) (PPN).

3.2.2. With $[PPh_4][BF_4]$

A mixture of **1a** (97 mg, 0.042 mmol) and $[PPh_4][BF_4]$ (39 mg, 0.92 mmol) in acetone (20 ml) was heated under reflux for 20 min. The solution was allowed to cool and filtered into vigorously stirred, deoxygenated distilled water (120 ml). The resulting precipitate was collected and subjected to TLC to give two dark-brown bands. The contents of these bands were identified from their ^{1}H NMR spectra ($CDCl_3$, 200 MHz) as follows: (a) band one was identified as a mixture of the (hydrido)(carbido)decaruthenium anion with the diruthenium and $[PPh_4]$ cations; (b) band two was found to contain a mixture of the dianion $[Ru_{10}(\mu_6\text{-}C)(CO)_{24}]^{2-}$ with the diruthenium and $[PPh_4]$ cations. In each case, the diruthenium cation was found to exist in both the head-to-head and head-to-tail orientations of the pyridyl moieties (hydride signals at δ −10.32 (Ru_2H, H–H), −10.78 (Ru_2H, H–T)).

3.3. Reaction between $[PPN]_2[Ru_{10}(\mu_6\text{-}C)(CO)_{24}]$ and HCl

Two drops of dilute HCl solution (approximately 30% in acetone) were added to $[PPN]_2[Ru_{10}(\mu_6\text{-}C)(CO)_{24}]$ (20 mg) in acetone (15 ml) and the reaction was monitored by IR spectroscopy. Peaks due to the dianionic cluster were seen to broaden as a dark precipitate separated. Stirring for 2 h resulted in the formation of a pale-brown solution and insoluble dark-brown precipitate. No IR spectral evidence for the formation of $[Ru_{10}(\mu\text{-}H)(\mu_6\text{-}C)(CO)_{24}]^-$ was found. Similar reactions with $HBF_4 \cdot Et_2O$ (a few drops of a dilute solution) and $DMA \cdot HPF_6$ (4 equiv.) resulted in trace amounts of the desired (hydrido) decaruthenium anion and a similar insoluble product.

*3.4. ^{13}C NMR spectroscopic data for **3a–5c***

*3.4.1. $[Ru_2(\mu\text{-}H)(\mu\text{-}NC_5H_4)_2(CO)_4(NC_5H_5)_2][Ru_{10}(\mu\text{-}H)(\mu_6\text{-}C)(CO)_{22}(PPh_3)_2]$ (**3a**)*

δ 381.5 (μ_6-C); 212.6, 211.4, 210.6, 210.1, 208.1, 200.8, 198.6 (d, J(CP) = 8 Hz), 191.7 (ratio 2:3:3:2:2:2:2:6, $Ru_{10}CO$); 197.5, 197.0 (ratio 1:1, Ru_2CO); 134.5–134.1 (m), 132.6–132.4 (m), 131.3, 129.3–129.2 (m) (aromatic C).

*3.4.2. $[Ru_2(\mu\text{-}H)(\mu\text{-}NC_5H_4)_2(CO)_4(NC_5H_5)_2][Ru_{10}(\mu\text{-}H)(\mu_6\text{-}C)(CO)_{21}(PPh_3)_3]$ (**4a**)*

δ 384.0 (μ_6-C); 214.5, 212.6, 212.2, 211.5, 209.9, 209.3, 201.3 (d, J(CP) = 8 Hz), 199.0, 192.8 (ratio 1:1:2:4:2:2:2:4:3, $Ru_{10}CO$), 197.4, 196.9 (Ru_2CO); 134.2 (m), 133.6, 133.5, 132.3 (d, J(CP) = 10 Hz), 131.8, 130.7, 129.9, 129.2–128.8 (m) (aromatic C).

*3.4.3. $[Ru_2(\mu\text{-}H)(\mu\text{-}NC_5H_4)_2(CO)_4(PPh_3)_2][Ru_{10}(\mu\text{-}H)(\mu_6\text{-}C)(CO)_{20}(PPh_3)_4]$ (**5c**)*

δ 386.0 (μ_6-C); 213.7, 213.2, 210.9, 201.9 (br), 199.7 (d, J(CP) = 15 Hz) (ratio 3:3:6:2:6, $Ru_{10}CO$); 134.4–134.2 (m), 132.4, 132.2, 130.3, 129.2, 129.0, 128.7, 128.5, 125.4 (aromatic C).

*3.5. Synthesis of $[PPh_4][Ru_{10}(\mu\text{-}H)(\mu_6\text{-}C)(CO)_{24}]$ (**1b**)*

A mixture of $Ru_3(\mu\text{-}H)(\mu\text{-}NC_5H_4)(CO)_{10}$ (50 mg, 0.075 mmol) and $[PPh_4][BF_4]$ (96 mg, 0.23 mmol) in chlorobenzene (10 ml) was heated under reflux for 50 min. The resulting black solution was allowed to come to room temperature and filtered through a filter aid to remove undissolved $[PPh_4][BF_4]$. The solution was taken to dryness in vacuo and the residue subjected to TLC. The contents of the resulting two main brown bands were obtained as black microcrystalline solids by crystallization from CH_2Cl_2–n-propanol. The first product (R_f = 0.6) was identified as **1b** (21 mg, 0.010 mmol, 45%). Anal. Found: C, 28.23; H, 0.99; $C_{49}H_{21}O_{24}Ru_{10}$ Calc.: C, 28.92; H, 1.04%. IR (CH_2Cl_2): ν(CO) 2052s, 2018(sh)m, 2008s cm^{-1}. ^{1}H NMR: δ 8.05–7.74 (m, 20H, PPh_4), −13.54 (s, 1H, RuH). ^{13}C NMR (213 K): δ 211.7, 209.8, 207.3, 190.2 (ratio 3:3:6:12, $Ru_{10}CO$); 136.3 (s), 135.6, 131.3 (2 × d, J(CP) = 12 Hz, PPh_4). ^{31}P NMR: δ 24.6 (s, PPh_4). The second product (R_f = 0.2) was identified as $[PPh_4]_2[Ru_{10}(\mu_6\text{-}C)(CO)_{24}]$ (1 mg, 0.0004 mmol, 8%). IR (CH_2Cl_2): ν(CO) 2025s, 2003m, 1982m cm^{-1}. ^{1}H NMR: δ 8.03–7.82 (m, PPh_4). ^{31}P NMR: δ 24.5 (s, PPh_4). Trace products were identified as unreacted starting material (yellow band, R_f = 0.9), **1a** (brown band, R_f = 0.65) and $[HRu_6(CO)_{18}]^-$ (orange band, R_f = 0.6) by comparison of the IR and ^{1}H NMR spectra.

*3.6. Reaction of **1b** with PPh_3*

*3.6.1. Synthesis of $[PPh_4][Ru_{10}(\mu\text{-}H)(\mu_6\text{-}C)(CO)_{23}(PPh_3)]$ (**2b**)*

Triphenylphosphine (approximately 1.3 mg, 0.0049 mmol) was added to a stirred solution of **1b** (10 mg, 0.0049 mmol) in acetone (10 ml). An IR spectrum after completion of the addition showed that reaction was

complete. The solution was taken to dryness and subjected to TLC. The products from the resulting two main green bands were crystallized from CH_2Cl_2–^iPrOH to afford green–black microcrystalline solids. The first product ($R_f = 0.5$) was identified as **2b** (9.0 mg, 0.0043 mmol, 82%). Anal. Found: C, 34.20; H, 1.65; $C_{66}H_{36}O_{23}P_2Ru_{10}$ Calc.: C, 34.93; H, 1.60%. IR (CH_2Cl_2): ν(CO) 2075w, 2046vs, 2015m, 1999m cm^{-1}. ^1H NMR: δ 7.90–7.84 (m, 4H, PPh_4), 7.72–7.61 (m, 16H, PPh_4), 7.57–7.52 (m, 15H, PPh_3), −11.54 (d, J(HP) = 8 Hz, 1H, RuH). ^{31}P NMR: δ 44.0 (s, 1P, RuP), 24.6 (s, 1P, PPh_4). The second product ($R_f = 0.4$) was identified as **3b** (1 mg, 0.0004 mmol, 8%) by comparison of the IR and NMR spectra.

3.6.2. Synthesis of $[PPh_4][Ru_{10}(\mu\text{-}H)(\mu_6\text{-}C)(CO)_{22}(PPh_3)_2]$ (3b)

Triphenylphosphine (22 mg, 0.084 mmol) was added to a stirred solution of **1b** (86 mg, 0.042 mmol) in acetone (15 ml) and the mixture was stirred for 60 min. An IR spectrum at this stage revealed the presence of some PPh_3-mono substituted decaruthenium anion. An additional portion of PPh_3 was added (5 mg, 0.103 mmol, 2.5 equiv. in total) and the mixture stirred until the IR spectrum indicated the absence of the monosubstituted anion, i.e. for a further 40 min. The solution was taken to dryness and the residue taken up in a minimum amount of acetone. TLC of the reaction mixture afforded a number of bands from which the two major products were crystallized from CH_2Cl_2–n-propanol to afford green–black microcrystalline solids. The first product ($R_f = 0.4$) was identified as **3b** (55 mg, 0.022 mmol, 52%). Anal. Found: C, 39.20; H, 1.94; $C_{83}H_{51}O_{22}P_3Ru_{10}$ Calc.: C, 39.81; H, 2.08%. IR (CH_2Cl_2): ν(CO) 2064m, 2040s, 2011s(sh), 2005vs, 1991m cm^{-1}. ^1H NMR: δ 7.94–7.56 (m, 50H, PPh_4 + PPh_3), −11.51 (d, J(HP) = 8 Hz, 1H, RuH). ^{31}P NMR: δ 51.8 (s, 1P, RuP), 43.0 (s, 1P, RuP), 24.5 (s, 1P, PPh_4). The second product ($R_f = 0.2$) was identified as **4b** by comparison of the IR and NMR spectra (20 mg, 0.0073 mmol, 17%).

3.6.3. Synthesis of $[PPh_4][Ru_{10}(\mu\text{-}H)(\mu_6\text{-}C)(CO)_{21}(PPh_3)_3]$ (4b)

Triphenylphosphine (20 mg, 0.078 mmol) was added to a stirred solution of **1b** (53 mg, 0.026 mmol) in acetone (10 ml) and the mixture stirred for 60 min. An IR spectrum at this stage revealed the presence of some PPh_3 monosubstituted decaruthenium anion. An additional portion of PPh_3 was added (8.0 mg, 0.11 mmol, 4.2 equiv. in total) and the mixture stirred for a further 20 min. The mixture was taken to dryness and taken up in a minimum amount of acetone. TLC of the reaction mixture afforded a number of trace bands and one major product (black band, $R_f = 0.2$). The latter was isolated as a green–black microcrystalline solid by trituration with light petroleum and identified as **4b** (34 mg, 0.012 mmol, 46%). Anal. Found: C, 42.97; H, 1.47; $C_{100}H_{66}O_{21}P_4Ru_{10}$ Calc.: C, 43.86; H, 2.43%. IR (CH_2Cl_2): ν(CO) 2049m, 2013s, 1999s, 1982m cm^{-1}. ^1H NMR: δ 8.00–7.99 (m, 4H, PPh_4), 7.88–7.84 (m, 16H, PPh_4), 7.69–7.48 (m, 45H, PPh_3), −11.53 (d, J(HP) = 7 Hz, 1H, RuH). ^{31}P NMR: δ 50.0, (s, 2P, RuP), 41.9 (s, 1P, RuP), 24.9 (s, 1P, PPh_4). Recrystallization from CH_2Cl_2–n-propanol afforded green–black crystals of **4b**. Found: C, 43.11; H, 2.08%. Two of the minor products were identified as **3b** and $[PPh_4][Ru_{10}(\mu\text{-}H)(\mu_6\text{-}C)(CO)_{20}(PPh_3)_4]$ **5b** by comparison of the IR and NMR spectra.

Acknowledgements

We thank the Australian Research Council for support of this work, Johnson-Matthey Technology Centre for the loan of ruthenium salts and Mr. C.J. Blake for assistance with the ^{13}C EXSY experiments. M.P.C. holds a UNE Postgraduate Research Scholarship. M.G.H. is an ARC Australian Research Fellow.

References

[1] M.P. Cifuentes, M.G. Humphrey, B.W. Skelton and A.H. White, *Organometallics, 14* (1995) 1536.
[2] M.P. Cifuentes, M.G. Humphrey, B.W. Skelton and A.H. White, *J. Organomet. Chem., 458* (1993) 211.
[3] M.P. Cifuentes, M.G. Humphrey, B.W. Skelton and A.H. White, *J. Organomet. Chem., 466* (1994) 211.
[4] M.P. Cifuentes, T.P. Jeynes, M.G. Humphrey, B.W. Skelton and A.H. White, *J. Chem. Soc., Dalton Trans.*, (1994) 925.
[5] T.P. Jeynes, M.P. Cifuentes, M.G. Humphrey, G.A. Koutsantonis and C.L. Raston, *J. Organomet. Chem., 476* (1994) 133.
[6] M.P. Cifuentes and M.G. Humphrey, in E.W. Abel, F.G.A. Stone and G. Wilkinson (eds.), *Comprehensive Organometallic Chemistry II*, Vol. 7, Elsevier, Oxford, 1995, Chapter 16.
[7] P.J. Bailey, E. Charalambous, J. Hoyle, B.F.G. Johnson, J. Lewis and M. McPartlin, *J. Chem. Soc., Chem. Commun.*, (1990) 1443.
[8] P.J. Bailey, M.A. Beswick, B.F.G. Johnson, J. Lewis, P.R. Raithby and M.C. Ramirez de Arellano, *J. Chem. Soc., Dalton Trans.*, (1992) 3159.
[9] P.J. Bailey, B.F.G. Johnson, J. Lewis, M. McPartlin and H.R. Powell, *J. Organomet. Chem., 377* (1989) C17.
[10] M.P. Cifuentes, M.G. Humphrey, B.W. Skelton and A.H. White, *Organometallics, 12* (1993) 4272.
[11] B.R. Cockerton and A.J. Deeming, *J. Organomet. Chem., 426* (1992) C36.
[12] D. Braga and F. Grepioni, *Organometallics, 11* (1992) 1256.
[13] D. Braga, F. Grepioni, S. Righi, B.F.G. Johnson, P. Frediani, M. Bianchi, F. Piacenti and J. Lewis, *Organometallics, 11* (1992) 706.
[14] A. Bashall, L.H. Gade, J. Lewis, B.F.G. Johnson, G.J. McIntyre and M. McPartlin, *Angew. Chem., Int. Edn. Engl., 30* (1991) 1164.
[15] C.R. Eady, B.F.G. Johnson, J. Lewis, M.C. Malatesta, P. Machin and M. McPartlin, *J. Chem. Soc., Chem. Commun.*, (1976) 945.

[16] P.F. Jackson, B.F.G. Johnson, J. Lewis, P.R. Raithby, M. McPartlin, W.J.H. Nelson, K.D. Rouse, J. Allibon and S.A. Mason, *J. Chem. Soc., Chem. Commun.*, (1980) 295.
[17] T. Chihara, Y. Matsuura and H. Yamazaki, *J. Chem. Soc., Chem. Commun.*, (1988) 886.
[18] E.C. Constable, B.F.G. Johnson, J. Lewis, G.N. Pain and M.J. Taylor, *J. Chem. Soc., Chem. Commun.*, (1982) 754.
[19] P.F. Jackson, B.F.G. Johnson, J. Lewis, M. McPartlin and W.J.H. Nelson, *J. Chem. Soc., Chem. Commun.*, (1982) 49.
[20] P.J. Bailey, L.H. Gade, B.F.G. Johnson and J. Lewis, *Chem. Ber., 125* (1992) 2019.
[21] D. Braga, K. Henrick, B.F.G. Johnson, J. Lewis, M. McPartlin, W.J.H. Nelson and J. Puga, *J. Chem. Soc., Chem. Commun.*, (1982) 1083.
[22] V. Dearing, S.R. Drake, B.F.G. Johnson, J. Lewis, M. McPartlin and H.R. Powell, *J. Chem. Soc., Chem. Commun.*, (1988) 1331.
[23] S.R. Drake, K. Henrick, B.F.G. Johnson, J. Lewis, M. McPartlin and J. Morris, *J. Chem. Soc., Chem. Commun.*, (1986) 928.
[24] R.J. Goudsmit, P.F. Jackson, B.F.G. Johnson, J. Lewis, W.J.H. Nelson, J. Puga, M.D. Vargas, D. Braga, K. Henrick, M. McPartlin and A. Sironi, *J. Chem. Soc., Dalton Trans.*, (1985) 1795.
[25] A.E. Derome, *Modern NMR Techniques for Chemistry Research*, Pergamon Press, Oxford, 1987, p. 240.
[26] M.I. Bruce, M.G. Humphrey, M.R. Snow, E.R.T. Tiekink and R.C. Wallis, *J. Organomet. Chem., 314* (1986) 311.
[27] V. Weerasuria, personal communication.
[28] D.F. Shriver and M.A. Drezdzon, *The Manipulation of Air Sensitive Compounds*, Wiley, New York, 1986.